Liquid Crystals
Publication details, including instructions for authors and subscription information:
http://www.informaworld.com/smpp/title~content=t713926090

Polarized states of hybrid aligned nematic layers

Grzegorz Derfel; Mariola Felczak

Online publication date: 11 November 2010

To cite this Article Derfel, Grzegorz and Felczak, Mariola(2002) 'Polarized states of hybrid aligned nematic layers', Liquid Crystals, 29: 7, 889 — 897
To link to this Article: DOI: 10.1080/02678290210143915
URL: http://dx.doi.org/10.1080/02678290210143915

LIQUID CRYSTALS, 2002, VOL. 29, NO. 7, 889–897

Taylor & Francis
Taylor & Francis Group

Polarized states of hybrid aligned nematic layers

GRZEGORZ DERFEL* and MARIOLA FELCZAK
Technical University of Łódź, Institute of Physics, ul. Wólczańska 219,
93-005 Łódź, Poland

(*Received 3 December 2001; in final form 17 February 2002; accepted 22 February 2002*)

Electric polarization arising in hybrid aligned nematic liquid crystal layers with rigid boundary conditions is studied numerically by solving the torques equation and Poisson equation. Three phenomena that give rise to the polarization are taken into account: flexoelectricity, surface polarization and adsorption of ions. The director orientation within the layer, as well as the distribution of electric potential and space charge density are calculated for layers deformed by an external magnetic field. The role of the ionic space charge is investigated. For a particular set of parameters of a model substance, the voltage arising between the layer surfaces varies from 10^{-1} V (in an extremely pure nematic) to 10^{-3} V (in material with a typical ion concentration). The surface polarization yields an additional voltage (of the order 10^{-2} V) nearly independent of the ion concentration. The effect of simultaneous flexoelectric polarization and ion adsorption is evidently different from a linear superposition of their separate contributions. The flexoelectric polarization leads to partial separation of ions of opposite signs. In the case of positive flexoelectric coefficients, a thin sublayer of positive charge arises at the planar-orienting boundary plate. The negative charge is displaced towards the homeotropically aligning plate. The magnitude of this effect increases with the magnetic field. The surface phenomena introduce additional subsurface charges.

1. Introduction

The electrical properties of nematic liquid crystals are related to the anisotropic electric polarizability of the mesogenic molecules, to the permanent dipole moments which they usually possess, to the ionic space charge which is practically unavoidable even in thoroughly purified materials and to the quadrupolar moment density connected with the quadrupolar form of the order parameter tensor. These properties are the origin of a variety of complex phenomena resulting in the polarization of nematic samples. Here we focus attention on the following three effects of this kind: flexoelectric polarization, surface polarization and ion adsorption.

Flexoelectric properties are quite common for liquid crystal compounds. Usually they are attributed to the asymmetrical shape of the mesogenic dipolar molecules [1]. In the case of non-polar molecules, they appear to be due to a gradient of the quadrupole moment density [2]. Electric polarization arises in a sample of nematic liquid crystal possessing flexoelectric properties whenever the director field in the sample contains splay or bend [1]. This case is known as the direct flexoelectric effect. Surface polarization may occur due to the adsorption of dipolar molecules resulting from the different chemical affinity of their ends for a substrate, or it may be caused by a spatial variation of the nematic ordering in a thin sublayer close to an interface (known as ordoelectric polarization [3]). The selective adsorption of ions of one sign (usually positive [4]) induces an electric field over a distance of the order of the Debye screening length from each of the surfaces. The ions of opposite signs are accumulated in the vicinity of the surfaces forming a double layer.

In this paper, hybrid aligned nematic layers with rigid director orientations at the surfaces are considered. One-dimensional distortions of the director distribution induced by an external magnetic field are taken into account. The flexoelectric polarization, which arises in the hybrid layer, contributes to the electric potential difference between the layer surfaces due to the asymmetry of the director distribution. The surface polarization and the ion adsorption may also lead to potential differences of comparable magnitude. The ionic space charge is redistributed due to the adsorption and to the interaction with the effective electric field and affects the potential distribution. One may expect that the director configuration in the sample is also influenced by interactions of the dielectrically anisotropic and polarized medium

*Author for correspondence; e-mail: gderfel@ck-sg.p.lodz.pl

Liquid Crystals ISSN 0267-8292 print/ISSN 1366-5855 online © 2002 Taylor & Francis Ltd
http://www.tandf.co.uk/journals
DOI: 10.1080/02678290210143915

with the electric fields induced by flexoelectricity and adsorption phenomena [5]. The charged regions appear in the electrically neutral sample. Sufficiently large ion concentrations can cause screening effects and suppress the potential differences. The properties of the nematic layer cannot be described by the linear superposition of the three polarizing phenomena mentioned above. This is mainly due to the non-linear coupling between the potential distribution and the ion concentration, and is related to the non-local character of the electric field [6].

In this paper, the above effects are investigated numerically. Our aims are as follows: (i) to compare the effects of surface polarization and ion adsorption with the flexoelectric effect, (ii) to calculate the space charge and electric potential distributions in the presence of these effects and to give quantitative examples of them, (iii) to determine the significance of the ion concentration for the electric potential difference, for the director distribution and for the net polarization of the layer. The geometry of the layers, the material parameters and the basic equations are given in the next section. The results of calculations are presented in § 3. Section 4 is devoted to a short discussion.

2. Method

2.1. *Geometry and parameters*

The nematic liquid crystal layer of thickness $d = 10\,\mu m$ was confined between two plates parallel to the xy plane in a Cartesian co-ordinate system and positioned at $z = \pm d/2$. The rigid director orientations, planar at $z = -d/2$ and homeotropic at $z = d/2$, assured the hybrid alignment. The director $\mathbf{n}$ was parallel to the yz plane. Its orientation was defined by the angle $\theta(z)$, measured between $\mathbf{n}$ and the y axis. The magnetic field of induction $\mathbf{B}$ was applied along the y or the z axis. The model substance was characterized by equal elastic constants $k_{11} = k_{33} = k = 10^{-11}$ N and a positive diamagnetic anisotropy $\Delta\chi$. The positive dielectric anisotropy $\Delta\varepsilon = \varepsilon_{\parallel} - \varepsilon_{\perp}$ was taken into account with the dielectric constant tensor ε having components $\varepsilon_{\perp} = 10$ and $\varepsilon_{\parallel} = 20$. In the following, reduced variables ζ and b defined by $z = \zeta d$ and $B = b(\pi/d)(k\mu_0/|\Delta x|)^{1/2}$ are used.

The flexoelectric properties were determined by equal flexoelectric coefficients $e_{11} = e_{33} = e$, varied in the range 0–3×10^{-11} C m^{-1}. The flexoelectric polarization vector $\mathbf{P}_f$ was expressed by the formula

$$\mathbf{P}_f = e_{11}\mathbf{n}(\nabla\mathbf{n}) - e_{33}\mathbf{n} \times (\nabla \times \mathbf{n}). \tag{1}$$

The surface polarization $\mathbf{P}_S$ was assumed to be induced by the ordo-electric mechanism which is due to the spatial variation of the nematic scalar order parameter $S(\zeta)$ taking place in the close vicinity to the layer walls. This approach was based on the experimental results obtained by Blinov *et al.* [7], who found non-zero surface polarization on the homeotropic as well as on the planar boundary plates. (The different chemical affinity of the ends of the molecules for a substrate would not give any surface polarization in the case of planar alignment.) The surface polarization value $P_S = |\mathbf{P}_S|$ was expressed by

$$P_S = \frac{3}{2} e_0 \frac{1}{d} \frac{dS}{d\zeta}\left(\sin^2\theta - \frac{1}{3}\right) \tag{2}$$

where e_0 is the quadrupolar coefficient [8]. It depends on the director orientation $\theta(\zeta)$ and therefore has different magnitudes P_P and P_H at the planar and homeotropic walls, respectively. We assumed that the order parameter varied exponentially in the subsurface region from $S_{surface}$ to S_{bulk} with the characteristic length L:

$$S(\zeta) = (S_{surface} - S_{bulk})\{\exp[-(\zeta + 0.5)/\lambda] + \exp[(\zeta - 0.5)/\lambda]\} + S_{bulk} \tag{3}$$

where $\lambda = L/d$. (The length $L = 50$ nm was chosen arbitrarily. Its exact value is not essential for the qualitative character of the phenomena studied.) The form of the $S(\zeta)$ function given by equation (3) is approximate and can be derived in the frame of a Landau–Ginzburg approach [9]. According to equations (2) and (3), the surface polarization decreases exponentially with distance from the boundaries according to the formula

$$P_S = P_P \exp[-(\zeta + 0.5)/\lambda] + P_H \exp[(\zeta - 0.5)/\lambda]. \tag{4}$$

It was significant only in the close vicinity of the surfaces where the changes of the calculated director orientation were negligible. The electric field induced by the surface polarization decayed over a distance of the order $3L$ from each surface. We used the values of P_P and P_H obtained from the relations

$$m_P = P_P L, \quad m_H = P_H L \tag{5}$$

where m_P and m_H are the effective dipole moments counted per unit area of the layer. (The inequality $L \ll d$ was applied to derive (5)). The magnitudes, as well as the senses of the vectors $\mathbf{m}_P$ and $\mathbf{m}_H$ were based on the results obtained in [7]: $\mathbf{m}_H(0, 0, m_H)$, $\mathbf{m}_P(0, 0, m_P)$, where $m_H = 4 \times 10^{-12}$ C m^{-1} and $m_P = 2 \times 10^{-12}$ C m^{-1}. Considerations analogous to those taken in [7] gave the relation $S_{surface} > S_{bulk}$, which resulted from the sign of $e_{11} + e_{33}$ and the senses of $\mathbf{m}_P$ and $\mathbf{m}_H$.

The ion concentration N was assumed to lie between 10^{18} m^{-3} and 10^{21} m^{-3} according to the typical electrical

conductivity $\kappa \approx 10^{-12}$–$10^{-10}\ \Omega^{-1}\ m^{-1}$ [10] and ionic mobility $\mu \approx 10^{-8}$–$10^{-7}\ m^2\ V^{-1}\ s^{-1}$ [11, 12]. The selective adsorption of positive ions was assumed. Their surface densities were equal on both plates, $\sigma_P = \sigma_H = \sigma$. The fraction of positive ions, which were adsorbed by the boundary surfaces, was characterized quantitatively by means of the parameter $a = 2\sigma/Nd$. In our calculations, σ reached $10^{14}\ m^{-2}$ for $N = 10^{20}\ m^{-3}$ which gave $a = 0.2$. Because of selective adsorption, the material in the bulk was not electrically neutral and potential differences appeared within the layer. The electric field originated by the adsorbed positive ions influenced the distribution of the remaining charges. The asymmetry of the director distribution and high electric anisotropy of the nematic provided some effective voltage between the boundary plates, even if $\sigma_P = \sigma_H$. This yielded a contribution to the net polarization of the layer. The ion adsorption influenced the bulk electrical properties of the sample due to the space charge redistribution.

2.2. *Basic equations*

The total free energy of the layer can be expressed as a sum of several contributions. They are due to curvature elasticity, dielectric anisotropy, flexoelectric properties, surface polarization, the external magnetic field and interaction of space charges with the intrinsic electric field:

$$F = \int_\tau (f_s + f_d + f_f + f_p + f_m + f_e)\,d\tau \tag{6}$$

where f_s, f_d, f_f, f_p, f_m and f_e denote the corresponding free energy densities, respectively and the integration is performed over the volume τ. They are given by the following general formulae:

$$f_s = \frac{1}{2}k(\nabla\ \mathbf{n})^2 + \frac{1}{2}k(\nabla \times \mathbf{n})^2 \tag{7}$$

$$f_d = -\frac{1}{2}\varepsilon_0 \mathbf{E}\ \ \mathbf{D} \tag{8}$$

$$f_f = -\mathbf{P}_f\ \ \mathbf{E} \tag{9}$$

$$f_p = -\mathbf{P}_S\ \ \mathbf{E} \tag{10}$$

$$f_m = -\frac{1}{2\mu_0}\mathbf{B}\ \ \hat{\boldsymbol{\chi}}\mathbf{B} \tag{11}$$

$$f_e = \rho V \tag{12}$$

where V is the electric potential, $\mathbf{E}$ is the electric field strength vector, $\mathbf{D}$ is the electric induction vector, $\hat{\boldsymbol{\chi}}$ denotes the diamagnetic susceptibility tensor and ρ is the space charge density.

According to the aforementioned assumptions, the formulae (7)–(10) become

$$f_s = \frac{1}{2d^2}k\left(\frac{d\theta}{d\zeta}\right)^2 \tag{13}$$

$$f_d = -\frac{1}{2d^2}\varepsilon_0(\varepsilon_\perp + \Delta\varepsilon \sin^2\theta)\left(\frac{dV}{d\zeta}\right)^2 \tag{14}$$

$$f_f = \frac{e}{d^2}\sin 2\theta \frac{d\theta}{d\zeta}\frac{dV}{d\zeta} \tag{15}$$

$$f_p = \frac{\exp(-0.5/\lambda)}{d\lambda}[m_P \exp(-\zeta/\lambda) + m_H \exp(\zeta/\lambda)]\left(\frac{dV}{d\zeta}\right). \tag{16}$$

The magnetic term (11) is replaced by

$$f_m = -\frac{1}{2}\frac{\pi^2}{d^2}kb^2 \sin^2\theta \tag{17 a}$$

when $\mathbf{B} \| z$, or by

$$f_m = -\frac{1}{2}\frac{\pi^2}{d^2}kb^2 \cos^2\theta \tag{17 b}$$

when $\mathbf{B} \| y$.

The ions in the nematic liquid are assumed to obey Boltzmann statistics. The concentrations of ions of both signs, denoted by $N_+(\zeta)$ and $N_-(\zeta)$, depend on the position in the sample. This distribution is governed by an ionic energy $\pm qV$, where q is the absolute value of the ionic charge. Therefore, $N_\pm(\zeta)$ depends on the potential distribution, which, on the other hand, is influenced by the ion distribution. For the layer containing N ion pairs per unit volume, they are given by

$$N_+(\zeta) = \frac{(1-a)N \exp(-V(\zeta)q/k_B T)}{\int_{-1/2}^{1/2} \exp(-V(\zeta)q/k_B T)\,d\zeta},$$

$$N_-(\zeta) = \frac{N \exp(V(\zeta)q/k_B T)}{\int_{-1/2}^{1/2} \exp(V(\zeta)q/k_B T)\,d\zeta} \tag{18}$$

where k_B is the Boltzmann constant and T is the absolute temperature. The adsorption of positive ions is represented in (18) by means of the coefficient $1-a$. The charge density in the layer is therefore expressed by

$$\rho(\zeta) = NqR(\zeta) \tag{19}$$

where

$$R(\zeta)=\frac{(1-a)\exp(-V(\zeta)q/k_{\mathrm{B}}T)}{\int_{-1/2}^{1/2}\exp(-V(\zeta)q/k_{\mathrm{B}}T)\,\mathrm{d}\zeta}-\frac{\exp(V(\zeta)q/k_{\mathrm{B}}T)}{\int_{-1/2}^{1/2}\exp(V(\zeta)q/k_{\mathrm{B}}T)\,\mathrm{d}\zeta}. \tag{20}$$

The equilibrium states of the layers are calculated by minimization of the total free energy. Standard variational methods give the set of two differential equations. The torques equation has the form

$$k\frac{\mathrm{d}^2\theta}{\mathrm{d}\zeta^2}+\frac{1}{2}\varepsilon_0\Delta\varepsilon\sin 2\theta\left(\frac{\mathrm{d}V}{\mathrm{d}\zeta}\right)^2+e\sin 2\theta\left(\frac{\mathrm{d}^2V}{\mathrm{d}\zeta^2}\right)\pm\frac{1}{2}\pi^2kb^2\sin 2\theta=0 \tag{21}$$

where '+' before the last component refers to $\mathbf{B}\parallel y$ and '−' to the $\mathbf{B}\parallel z$ case. The electrostatic equation is

$$Nqd^2R(\zeta)+\varepsilon_0(\varepsilon_\perp+\Delta\varepsilon\sin^2\theta)\frac{\mathrm{d}^2V}{\mathrm{d}\zeta^2}+\varepsilon_0\Delta\varepsilon\sin 2\theta\frac{\mathrm{d}V}{\mathrm{d}\zeta}\frac{\mathrm{d}\theta}{\mathrm{d}\zeta}-2e\cos 2\theta\left(\frac{\mathrm{d}\theta}{\mathrm{d}\zeta}\right)^2-e\sin 2\theta\frac{\mathrm{d}^2\theta}{\mathrm{d}\zeta^2}+\frac{\exp(-0.5/\lambda)}{\lambda^2}\times[m_{\mathrm{P}}\exp(-\zeta/\lambda)-m_{\mathrm{H}}\exp(\zeta/\lambda)]=0. \tag{22}$$

The boundary conditions for $\theta(\zeta)$ are $\theta(-1/2)=0$, $\theta(1/2)=\pi/2$. The boundary conditions for the potential are determined by the equations

$$\left.\frac{\mathrm{d}V}{\mathrm{d}\zeta}\right|_{\zeta=\pm 1/2}=\frac{e\sin 2\theta(\pm 1/2)(\mathrm{d}\theta/\mathrm{d}\zeta)|_{\zeta=\pm 1/2}+P_{\mathrm{S}}(\pm 1/2)d\pm\sigma d}{\varepsilon_0[\varepsilon_\perp+\Delta\varepsilon\sin^2\theta(\pm 1/2)]} \tag{23a}$$

which read

$$\frac{\mathrm{d}V}{\mathrm{d}\zeta}=\frac{m_{\mathrm{P}}/\lambda-\sigma_{\mathrm{P}}d}{\varepsilon_0\varepsilon_\perp} \tag{23b}$$

for $\zeta=-1/2$, and

$$\frac{\mathrm{d}V}{\mathrm{d}\zeta}=\frac{m_{\mathrm{H}}/\lambda+\sigma_{\mathrm{H}}d}{\varepsilon_0\varepsilon_\parallel} \tag{23c}$$

for $\zeta=1/2$. The lower boundary plate is assumed to be grounded: $V(-1/2)=0$.

Equations (21) and (22) were solved numerically. The functions $\theta(\zeta)$ and $V(\zeta)$ were obtained and the space charge density $\rho(\zeta)$ was calculated.

Charged regions arise as a consequence of separation of positive and negative ions even within the electrically neutral layer (i. e. in the absence of ion adsorption). The magnitude of the corresponding separated charge per unit area is defined for the neutral layers by the quantity

$$Q=\int_{-1/2}^{1/2}|\rho(\zeta)|\,\mathrm{d}\zeta. \tag{24}$$

3. Results

The director configuration (described by the angle $\theta(\zeta)$), the electric potential distribution $V(\zeta)$ and the volume space charge density distribution $\rho(\zeta)$ were calculated from the torques equation (21) and the Poisson equation (22). The influence of the magnetic field, of the ion concentration, of the surface polarization and of the ion adsorption on these distributions was studied.

The non-uniform director distribution in the hybrid layer is sufficient for the appearance of interesting polarization phenomena. The situation in the absence of the magnetic field is briefly described in § 3.1. The stronger deformations induced by the field enhance the magnitude of these effects. The detailed description of the results for the field applied perpendicular to the layer is presented in § 3.2. The case for the field parallel to the layer (and to the director plane) is described qualitatively in § 3.3.

3.1. $\boldsymbol{B}=0$

In this subsection, we restrict our attention to the pure flexoelectric polarization. It arises in the absence of the magnetic field due to the hybrid structure of the layer. For a high ion concentration ($N=10^{20}\ \mathrm{m}^{-3}$), the angle θ varies linearly with ζ. This coincides with the $\theta(\zeta)$ function expected for the hybrid structure in the one-constant approximation and does not reveal any evidence of the flexoelectric effect. For a low ion concentration ($N=10^{18}\ \mathrm{m}^{-3}$), a subtle deviation from linearity of the $\theta(\zeta)$ function can be noted. Nevertheless, in both cases, an approximate symmetry is evident in the potential and space charge distributions as exemplified in figure 1. The function $f(\zeta)=V(\zeta)-U/2$ (where U denotes the voltage arising between the layer boundaries) is nearly odd. Small deviations from perfect symmetry are due to the high dielectric anisotropy and its interaction with the electric field of flexoelectric origin. The positive ions are partially removed from the region $0<\zeta<0.5$, whereas the negative ions are displaced from the other half of the layer. The separation of ions occurs symmetrically, i.e. their concentrations are connected by a relation $N_+(\zeta)\approx N_-(-\zeta)$. As a result, the charge distribution is described by the nearly odd $\rho(\zeta)$ function. The potential

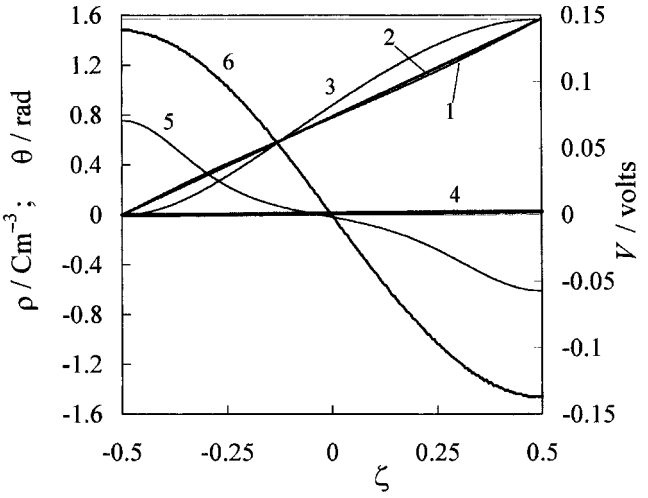

Figure 1. Distributions of the orientation angle $\theta(\zeta)$ (curves 1, 2, left scale), electric potential $V(\zeta)$ (curves 3, 4, right scale) and space charge density $\rho(\zeta)$ (curves 5, 6, left scale) in the hybrid aligned nematic layer for $N = 10^{18}$ m^{-3} (curves 1, 3, 5) and $N = 10^{20}$ m^{-3} (curves 2, 4, 6). Please note that the units for θ and ρ on the left scale coincide.

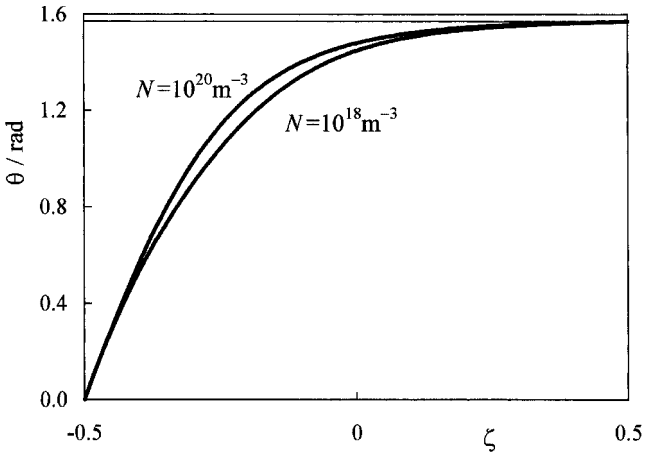

Figure 2. Influence of the ion concentration N on the director orientation in the layer deformed by the magnetic field $b = 2$; $e = 30$ pC m^{-1}.

and charge distributions caused by the surface effects are superimposed on the functions mentioned above. The details of these effects are described in the next section.

The influence of the ion concentration is evident. The potential differences are drastically suppressed at $N = 10^{20}$ m^{-3} in comparison with the case of $N = 10^{18}$ m^{-3}. The space charge distributions are affected to a lesser extent.

3.2. $\boldsymbol{B} \| z$

3.2.1. *Director distribution*

The director configuration in the hybrid aligned layer can be affected by the flexoelectric properties of the nematic substance, due to the interaction between the flexoelectric polarization and the dielectric anisotropy [5]. The ionic space charge influences this effect, since it may compensate the flexoelectric polarization.

In our layers, the change of the director distributions caused by the flexoelectricity is rather small and significant only at low ion concentrations ($N = 10^{18}$ m^{-3}). High ion concentrations ($N = 10^{20}$ m^{-3}) cancel this influence due to the screening effect of the ions. The resulting director distribution is identical to that obtained for a non-flexoelectric nematic. These relations are illustrated in figure 2 by means of $\theta(\zeta)$ functions plotted for the reduced magnetic field $b = 2$. The surface polarization does not exert any remarkable effect on the director distribution either for $N = 10^{18}$ m^{-3} or for $N = 10^{20}$ m^{-3}. The same applies to the surface adsorption with $a = 0.2$.

3.2.2. *Electric potential distribution*

All three phenomena leading to the polarization of the sample induce the electric potential differences in the layer and give rise to a voltage U between the layer boundaries. In our case, the greatest voltage arises at low ion concentrations as a consequence of the flexoelectric polarization resulting from the distortion of the director field in the hybrid structure. Its value is of the order 10^{-1} V. In figure 3, examples of the potential distribution $V(\zeta)$ are presented (curves 1 and 6). At a high ion concentration $N = 10^{20}$ m^{-3}, the potential differences due to the flexoelectricity are strongly suppressed. In strong magnetic fields, the flexoelectric potential is almost constant in the affected part of the layer due to the nearly uniform director distribution in this region.

In the absence of surface phenomena, the form of the equations (21), (22) and (23) (for given material properties k, e, $\Delta\varepsilon$, and the magnetic field b) does not change with N or d if only the quantity Nd^2 remains constant. In consequence, the solutions $\theta(\zeta)$ and $V(\zeta)$ are valid for various layers with the same Nd^2. Therefore, the dependence of U on ion concentration can be presented in a universal form including its dependence on thickness. Corresponding plots of the functions $U(Nd^2)$ are presented in figure 4 (curves 1–3). The voltage U decreases with ion concentration or with thickness of the layer. The highest values are obtained at low concentrations or in thin layers. For instance, in the layer of thickness $d = 10\,\mu$m filled with thoroughly purified material containing 10^{18} ion pairs per m^3, U reaches 0.22 V at $b = 1$. In the case of a typical nematic with $N = 10^{20}$ m^{-3}, U can still have a noticeable value of 0.02 V at the same thickness if a sufficiently high field is applied, e.g. $b = 4$. The highest U value found within our limits of parameters is 0.23 V for an insulating nematic. The effect of

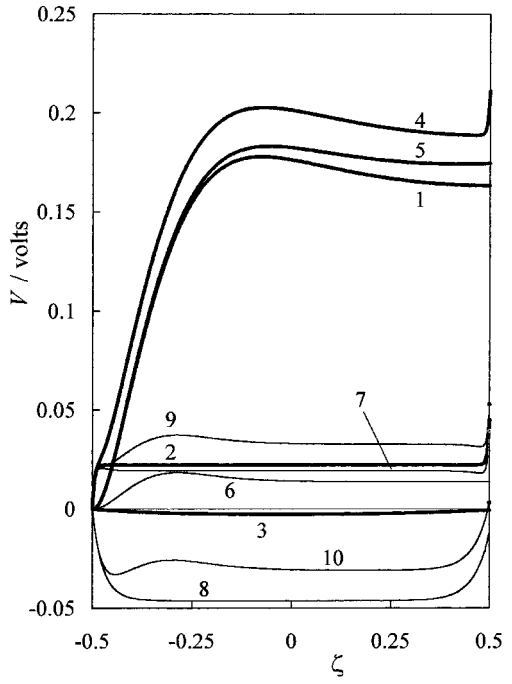

Figure 3. Potential distribution $V(\zeta)$ for two ion concentrations $N = 10^{18}$ m^{-3} (curves 1–5) and $N = 10^{20}$ m^{-3} (curves 6–10); $b = 2$, $e = 30$ pC m^{-1}. Curves 1, 6—pure flexoelectric effect; curves 2, 7—pure surface polarization; curves 3, 8—pure ionic adsorption with $a = 0.2$; curves 4, 9—flexoelectric effect in the presence of surface polarization; curves 5, 10—flexoelectric effect in the presence of ionic adsorption.

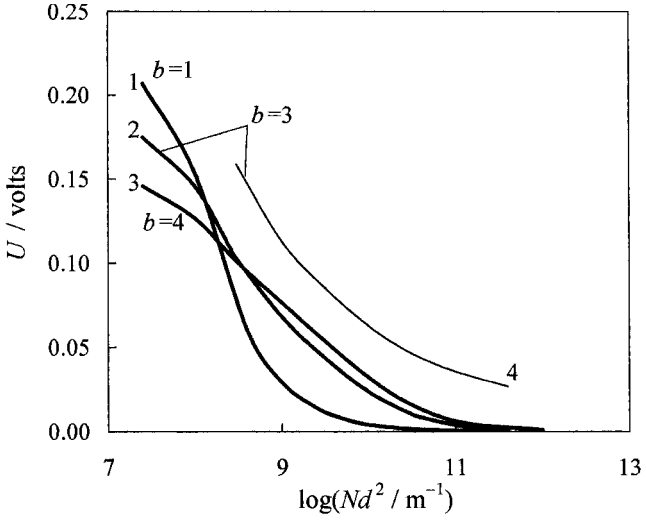

Figure 4. Voltage U between the boundaries of the layer as a function of Nd^2 for various magnetic field inductions b; $e = 30$ pC m^{-1}. Thick lines—pure flexoelectric effect; thin line—flexoelectric effect in the presence of surface polarization for $d = 10$ μm.

a magnetic field is illustrated in figure 5 (curves 1–4). The voltage U decreases with b for low N and increases with b for high N. For given b and N values, the voltage

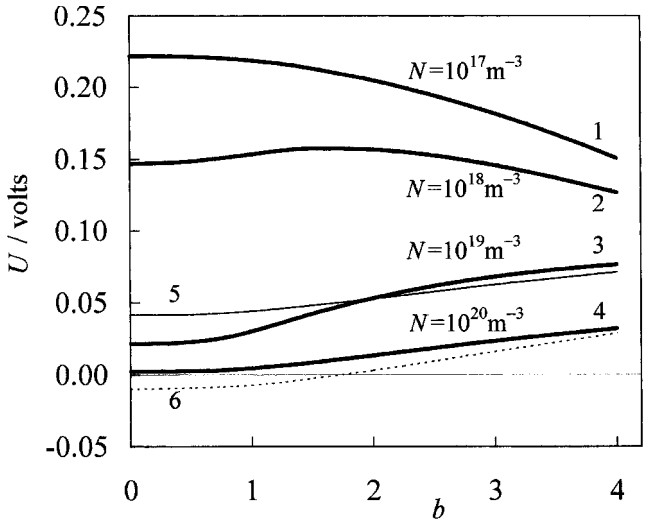

Figure 5. Voltage U as a function of magnetic field induction b; $e = 30$ pC m^{-1}. Thick lines (1–4)—pure flexoelectric effect; thin line—flexoelectric effect in the presence of surface polarization, $N = 10^{20}$ m^{-3}; dotted line—flexoelectric effect in the presence of ionic adsorption, $N = 10^{20}$ m^{-3}, $a = 0.2$.

U is nearly proportional to the flexoelectric coefficient e as exemplified in figure 6 (curves 1 and 2).

The potential differences produced by the surface polarization are due to the electric field that arises in the thin boundary regions. They are presented in figure 3 for a non-flexoelectric nematic with low and high ion concentrations (curves 2 and 7). It is evident that the potential distributions in the flexoelectric material with surface polarization (curves 4 and 9) are approximately

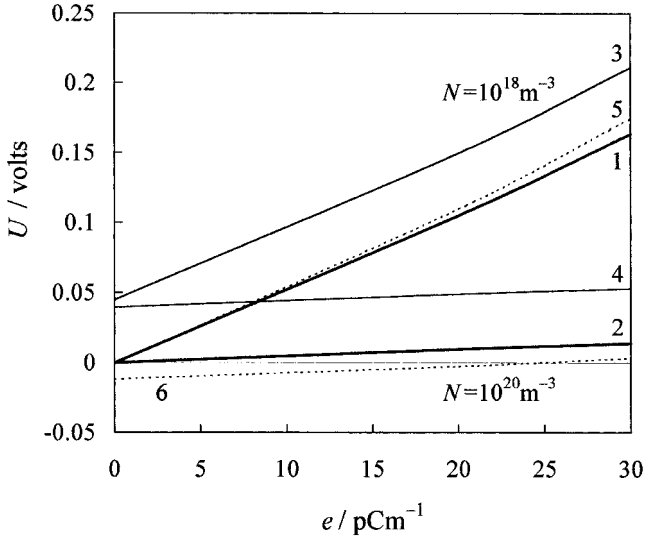

Figure 6. Voltage U as a function of the flexoelectric coefficient e for two ion concentrations, $b = 2$. Thick lines—pure flexoelectric effect; thin lines—flexoelectric effect in the presence of surface polarization; dotted lines—flexoelectric effect in the presence of ionic adsorption, $a = 0.2$.

equal to the sum of the distributions found for pure surface polarization and pure flexoelectric polarization effects. The same concerns the voltages due to these effects, as can be seen in figure 6. In the cases considered in figures 3–6, the surface polarization enhances the voltage of flexoelectric origin by about 0.05 V. This excess of voltage is almost independent of N, b and e as illustrated in figure 4 (curve 4), figure 5 (curve 5) and figure 6 (curves 3 and 4), respectively. For high N, it can exceed the flexoelectric voltage. The excess of voltage is proportional to the sum $m_P + m_H$.

The potential distribution induced by the surface adsorption is slightly asymmetrical with respect to $\zeta = 0$ which results in some low voltages. Curves 3 and 8 in figure 3 show the potential distributions induced in a non-flexoelectric nematic layer free from surface polarization, when the fraction $a = 0.2$ of all positive ions is adsorbed in equal amounts on both surfaces. The corresponding surface densities of ions are 10^{12} and 10^{14} for $N = 10^{18}$ and 10^{20} m^{-3}, respectively and result in significantly different potential distributions. The thickness of the regions in which the electric field has significant strength is comparable to the Debye length. It amounts to several tenths of a micron for $N = 10^{20}$ m^{-3}. Thus the electric field is limited to the thin regions at the boundaries. For $N = 10^{18}$ m^{-3} a weak electric field extends over the whole layer. A mutual correlation between the ionic adsorption and flexoelectricity can be noted. The potential difference arising in the presence of both effects is not equal to the sum of the $V(\zeta)$ distributions occurring for each of them separately. This is especially evident for low N (compare curves 1, 3 and 5 in figure 3). The other manifestation of this effect is shown in figure 6, where the influence of adsorption on the flexoelectric voltage, measured by the difference between curves 1 and 5 (or 2 and 6), varies with the value of the flexoelectric coefficient e. The influence of ion adsorption on the voltage U depends on b, which also reflects its coupling with the flexoelectric polarization (curve 6 in figure 5). The ion concentration N also affects the magnitude of this influence.

3.2.3. *Space charge distribution*

The polarization of the layer is connected with partial separation of ions of opposite signs.

The flexoelectric polarization enhances the positive ion concentration in the vicinity of the planar boundary. Simultaneously, a portion of negative ions is displaced from this region towards the middle of the layer. As a result, the space charge arises; its density distribution, $\rho(\zeta)$, is shown in figure 7 by curve 1. The thin layer of positive charges adjacent to the planar oriented plate is built up and a layer of negative charges is formed in its neighbourhood. The rest of the sample is electrically neutral. The stronger distortions induced by a higher magnetic field enhance this effect.

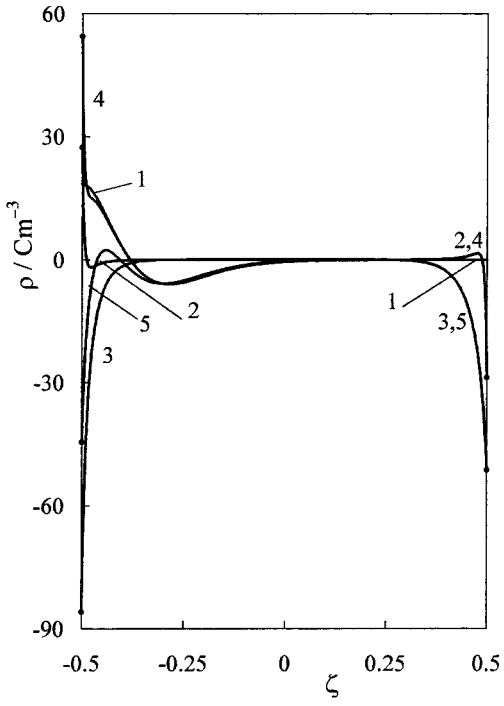

Figure 7. Space charge distribution $\rho(\zeta)$, $e = 30$ pC m^{-1}, $N = 10^{20}$ m^{-3}, $b = 2$. Curve 1—pure flexoelectric effect; curve 2—pure surface polarization; curve 3—pure ionic adsorption, $a = 0.2$; curve 4—flexoelectric effect in the presence of surface polarization; curve 5—flexoelectric effect in the presence of ionic adsorption.

The surface polarization considered in our work removes part of the positive ions from the vicinity of the homeotropic boundary and accumulates them at the planar plate. On the other hand, a thin sublayer at the homeotropic plate is enriched in negative ions which are removed from the neighbourhood of the planar plate. This charge redistribution yields very thin layers of positive and negative charges at $\zeta = -0.5$ and $\zeta = 0.5$, respectively, shown by curve 2 in figure 7. In the presence of both flexoelectric and surface polarizations, the corresponding charges are superimposed (curve 4).

In the presence of ions adsorption, the concentration of positive ions is strongly reduced in the vicinity of the boundaries, whereas the concentration of negative ions is strongly enhanced in the subsurface regions. As a result, clouds of negative charges accumulate at both plates (curve 3 in figure 7). They strongly affect the space charge distribution corresponding to the flexoelectric polarization (figure 7, curve 5).

The charge separated by the flexoelectric effect, counted per unit area of the layer and measured by the quantity Q, formula (24), depends on the magnetic field (thick curves in figure 8). For a low ion concentration

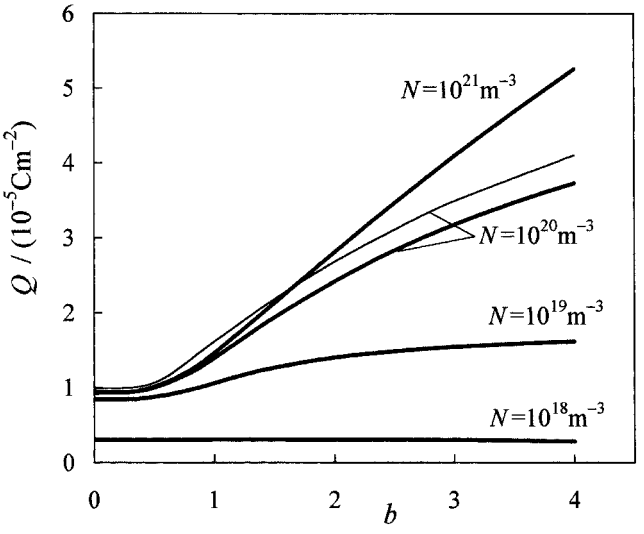

Figure 8. Separated charge Q as a function of the reduced magnetic induction b for various ion concentrations; $e = 30\ \mathrm{pC\ m^{-1}}$. Thick lines—pure surface polarization; thin line—flexoelectric effect in the presence of surface polarization.

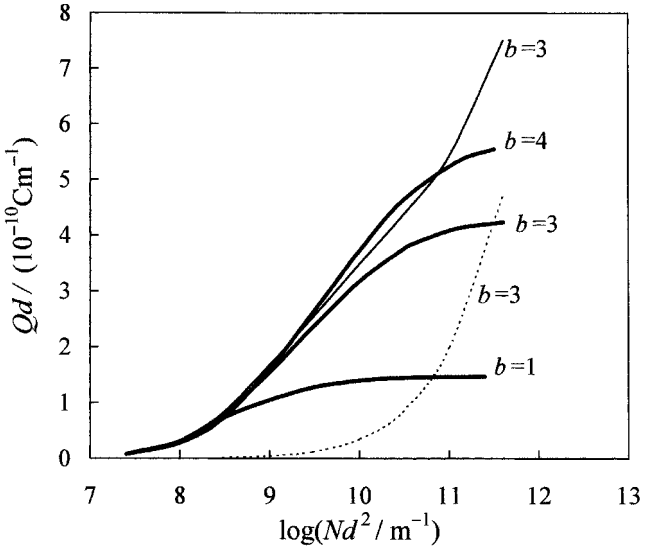

Figure 9. Relation between separated charge and ion concentration illustrated by the functions $Qd(Nd^2)$ for various magnetic fields. Thick lines—pure flexoelectric effect, $e = 30\ \mathrm{pC\ m^{-1}}$; thin line—flexoelectric effect in the presence of surface polarization; dashed line—pure surface polarization, $d = 10\ \mu\mathrm{m}$.

($N = 10^{18}\ \mathrm{m^{-3}}$), Q has an almost constant value $Q \approx 3.2 \times 10^{-6}\ \mathrm{C\ m^{-2}}$ which is equal to Nqd. This means that the flexoelectric polarization arising in the hybrid structure is sufficient for separation of the whole ionic charge even in the absence of the field. The essential part of the flexoelectric polarization remains uncompensated and gives rise to the voltage U. For $N = 10^{19}\ \mathrm{m^{-3}}$, the saturation of Q, due to complete ion separation, begins at $b = 1.5$; for $N = 10^{20}\ \mathrm{m^{-3}}$ it does not appear below $b = 4$. The charge per unit area of the layer reaches $4 \times 10^{-5}\ \mathrm{C\ m^{-2}}$ at $N = 10^{20}\ \mathrm{m^{-3}}$ and $e = 3 \times 10^{-11}\ \mathrm{C\ m^{-1}}$. It is nearly proportional to e. For low ion concentrations, the tendency to saturation of the $Q(e)$ dependence can be noted, i.e. Q approaches the value Nqd.

According to the remarks made in § 3.2.2, for the sample which is electrically neutral and free from surface polarization, the dependence of Q on the ion concentration and thickness can be illustrated by the plots of the quantity Qd as a function of Nd^2 (figure 9). The latter relation results from the expression for Q derived from equations (19), (20) and (24):

$$Q = Nqd \int_{-1/2}^{1/2} |R(\zeta)|\, \mathrm{d}\zeta. \tag{25}$$

The quantity dependent on Nd^2 can be obtained by multiplying both sides of equation (25) by d. For a given d, Q increases with N and saturates. This effect appears when the whole polarization in the layer is compensated by the redistributed charges, and this is clearly evident at low fields. The saturation of the Qd value indicates also that Q decreases with d for a given ion concentration. This reflects the smaller flexoelectric polarization as a consequence of weaker deformation of the director field.

The surface polarization gives its own contribution to the separated charges. This is illustrated in figure 8 for $N = 10^{20}\ \mathrm{m^{-3}}$, by the thin line. For higher concentrations, the charge separated by the surface polarization can have significant magnitudes. For a given d, the Q value strongly increases with N, which is exemplified by the dotted line in figure 9. The charge separated in the presence of flexoelectric and surface polarizations, presented by the thin line in figure 9, is approximately equal to the sum of the contributions due to both effects. However, this approximation becomes worse at higher N.

3.3. $\boldsymbol{B} \| \boldsymbol{y}$

The nearly symmetrical spatial dependences of the electric potential and space charge density described in § 3.1 are distorted by the magnetic field $\mathbf{B} \| \mathbf{y}$ in a manner analogous to the case for $\mathbf{B} \| \mathbf{z}$. As a result, the corresponding characteristics of the pure flexoelectric effects have analogous properties, namely, $\rho(\zeta)_{\mathbf{B}\|\mathbf{y}}$ is approximately equal to $-\rho(-\zeta)_{\mathbf{B}\|\mathbf{z}}$, whereas $V(\zeta)_{\mathbf{B}\|\mathbf{y}}$ is close to $[U - V(-\zeta)]_{\mathbf{B}\|\mathbf{z}}$. All the relations considered in § 3.2, i.e. $U(Nd^2)$, $U(b)$, $U(e)$, $Q(b)$, $Qd(Nd^2)$ have analogous forms to that shown in figures 4–6 and 8–9. The minor differences are due to the different roles of the electric field $\mathbf{E} \| \mathbf{z}$ existing in the layer. In the present case, this field counteracts the magnetic field-induced distortion of the director distribution.

The surface effects have approximately the same influence since they do not depend on the direction of the magnetic field. The small differences result from different director distributions.

4. Discussion

A model for a flexoelectric nematic layer in the presence of surface polarization and ion adsorption has been studied numerically in order to estimate the relative magnitudes of the effects caused by these phenomena. A similar approach was applied in [13] where the role of ions in the hybrid layer in the presence of a bias voltage was studied and the surface phenomena were neglected. In our paper, the properties of the layer are characterized by the calculated distributions of the electric potential, space charge density and director orientation angle. Experimental determination of these quantities seems to be very difficult or even impossible.

The values of the layer parameters were chosen to assure the evident and significant effects. They remain in the ranges determined experimentally for real liquid crystals, [9–11, 14], although some of them are known only from very few or uncertain measurements. In particular, the positive sign of the sum of the flexoelectric coefficients was adopted and a wide range of its variation was used. The range covers a part of existing experimental data [14] which is controversial not only in magnitude but also in sign. The non-flexoelectric nematic was also considered in order to illustrate effects due to pure surface phenomena, although flexoelectricity seems to be common in liquid crystals. Negative flexoelectric coefficients would give a reversed sign of the flexoelectric polarization.

Rigid boundary director orientations $\theta(-1/2) = 0$, $\theta(1/2) = \pi/2$ were assumed. Therefore the influence of the electric fields arising at the boundaries on the director adjacent to them, predicted in [15], was ignored.

The role of the ion concentration has been illustrated. At high concentrations, the flexoelectric polarization is compensated by the ions, whereas the surface polarization seems to be weakly sensitive to their presence. High ion concentrations give rise to significant surface densities of adsorbed ions, which may lead to high net polarization of the layer. The asymmetry of the layer gives rise to the voltage between the boundary plates, although the densities of the ions adsorbed on both boundaries are assumed equal. This effect can be explained by comparison of equations (23 *b*) and (23 *c*). They impose different boundary conditions, even when $e = 0$, $m_P = m_H = 0$ and $\sigma_P = \sigma_H$. The voltage would be significantly larger if the adsorbing surfaces were not identical.

The significant number of parameters which determine the properties of the layers being considered give rise to rather complex behaviour. The polarization effects of different nature are mutually correlated which makes the prediction of their coexistence difficult.

References

[1] Meyer, R. B., 1969, *Phys. Rev. Lett.*, **22,** 918.
[2] Prost, J., and Marcerou, J. P., 1977, *J. Phys. (Paris)*, **38,** 315.
[3] Barbero, G., Dozov, I., Palierne, J. F., and Durand, G., 1986, *Phys. Rev. Lett.*, **56,** 2056.
[4] Barbero, G., Zvezdin, A. K., and Evangelista, L. R., 1999, *Phys. Rev. E*, **59,** 1846.
[5] Deuling, H. J., 1978, in *Liquid Crystals*, edited by L. Liebert (New York: Academic Press), pp. 77–107.
[6] Dozov, I., Barbero, G., Palierne, J. F., and Durand, G., 1986, *Europhys. Lett.*, **1,** 563.
[7] Blinov, L. M., Barnik, M. I., Ohoka, H., Ozaki, M., Shtykov, N. M., and Yoshino, K., 2001, *Eur. Phys. J. E*, **4,** 183.
[8] Durand, G., 1990, *Physica A*, **163,** 94.
[9] Barbero, G., and Evangelista, L. R., 2001, *An Elementary Course on the Continuum Theory for Nematic Liquid Crystals* (Singapore: World Scientific), pp. 107–113.
[10] Naemura, S., and Sawada, A., 2000, *Mol. Cryst. liq. Cryst.*, **346,** 155.
[11] Derfel, G., and Lipiński, A., 1979, *Mol. Cryst. liq. Cryst.*, **55,** 89.
[12] Yamashita, M., and Amemiya, Y., 1978, *Jpn. J. appl. Phys.*, **17,** 1513.
[13] Ponti, S., Ziherl, P., Ferrero, C., and Zumer, S., 1999, *Liq. Cryst.*, **26,** 1171.
[14] Petrov, A. G., 2001, in *Physical Properties of Liquid Crystals: Nematics*, edited by D. A. Dunmur, A. Fukuda, and G. R. Luckhurst (London: INSPEC), pp. 251–264.
[15] Barbero, G., Evangelista, L. R., and Madhusudana, N. V., 1998, *Eur. Phys. J. B*, **1,** 327.